The Monte Carlo Method: Versatility Unbounded In A Dynamic Computing World
Chattanooga, Tennessee, April 17–21, 2005, on CD-ROM, American Nuclear Society, LaGrange Park, IL (2005)

STUDY OF SECONDARY PARTICLES PRODUCED BY 250 MeV PROTONS ON VARIOUS TARGETS

Hranitzky C. and Rollet S.
ARC Seibersdorf research GmbH
2444 Seibersdorf, AUSTRIA
Christian.Hranitzky@arcs.ac.at; Sofia.Rollet@ arcs.ac.at

Brandl A.
Nuclear Engineering Seiberdorf
2444 Seibersdorf, AUSTRIA
Alexander.Brandl@arcs.ac.at

ABSTRACT

MedAustron is a major Austrian project for a new medical proton and carbon ion accelerator facility. To ensure radiation safety for personnel, patients, and third persons involved in the hadron therapy treatment, detailed radiation protection related investigations especially for worst-case scenarios are necessary. In this study, two prominent Monte Carlo computer codes, FLUKA and MCNPX, are used for simulating 250 MeV proton beam irradiations of various targets representing beam-line components and the patient. The main goal of the study is the characterization of the secondary particle radiation fields and related uncertainties in the vicinity of the target. The total secondary particle yield is dominated by neutrons and photons with up to one emitted particle per primary incident proton. The angular neutron emission distribution is clearly peaked in forward direction, whereas for photons it is isotropic. Resulting ambient dose equivalent values in the unshielded environment were calculated and compared for six different target materials. The maximum dose equivalent rate (7 mSv/h at 5 m) was calculated for the copper target in forward scattering direction. The maximum difference (40% for secondary neutrons) between FLUKA and MCNPX results was observed for the tissue target in backward scattering direction. In general, higher dose values and different spectral and angular fluence distributions are produced by metal targets as compared to tissue-equivalent targets.

Key Words: MedAustron, Proton therapy, Radiation protection, Monte Carlo simulations

1 INTRODUCTION

MedAustron is a major Austrian research project for a medical proton and carbon ion therapy facility. The final design study of the MedAustron project [1] was recently published and agreed to by the Austrian government. Besides technical, medical, epidemiological, and economical parts the design study contains radiation protection related issues including necessary studies for normal operation and worst-case scenarios.

This work deals with basic investigations of secondary particle radiation fields produced around various targets bombarded by protons. As the maximum energy of the MedAustron proton therapy accelerator is in the range of 250 MeV, this is also the proton beam energy chosen

for the simulation study presented in this paper. The results of the target emitted radiation fields and calculated dose equivalents can thus be viewed as a worst case study.

Monte Carlo simulations of pencil beam irradiations of six target materials representing beam-line structures and the patient are carried out. Secondary particles such as neutrons, photons, and protons are investigated. The secondary particle fluence and particle energy distribution is detected in the unshielded vicinity of the targets. The total number of secondary particles as well as the angular and spectral distributions is calculated and directly compared for two prominent Monte Carlo transport codes, MCNPX [2] and FLUKA [3]. Resulting H*(10) ambient dose equivalent distributions outside the different targets are presented for the three main scattering directions, i.e. the forward, lateral, and backward directions. At the end, the influence of the geometrical target specifications on the secondary radiation emission is briefly discussed.

2 SIMULATION METHODS

The pencil beam geometry of the various target irradiations is modeled by a parallel beam of protons homogeneously distributed over a 1 mm diameter circular area. In this computer simulation study, simple cylindrical target geometries are used for simulating facility components such as magnets, beam dumps or shielding structures. The beam is impinging at normal incidence on the center of the plane surface of the target cylinder. This allows using the system's cylindrical symmetry for improved sampling. The targets are centered on the coordinate system’s origin and surrounded by vacuum.

A number of target materials are investigated, namely iron (Fe), aluminum (Al), copper (Cu), AISI 316LN stainless steel (Steel), and ICRU ordinary heavy concrete (Conc.). As a comparison to the former study by Brandl et al. [4], irradiation of the patient is also simulated using a cylindrical ICRU-4-element tissue (Tiss.) target. All target parameter values are shown in Table I.

Table I. Target specifications: material, density, 250 MeV proton stopping range, thickness, and elemental composition

Target	Density [g/cm3]	Range [cm]	Thickness [cm]	Composition Z:mass fraction
Tiss.	1.00	37.35	42.0	1:10.12%, 6:11.1%, 7:2.6%, 8:76.183%
Fe	7.87	6.93	7.5	26:100%
Al	2.699	17.99	22.0	13:100%
Cu	8.96	6.32	7.5	29:100%
Steel	7.87	-	7.5	6:0.03%, 7:0.13%, 14:1%, 15:0.045%, 16:0.03%, 24:17%, 25:2%, 26:65.3055%, 27:2.5%, 28:12%
Conc.	2.30	-	42.0	1:0.673%, 8:55.481%, 14:43.846%

The thickness of the targets is chosen to represent “thick” target irradiation conditions. Thicknesses just above the tabulated values of material’s stopping ranges of the ICRU [5] are chosen for producing maximum secondary particle emission from the target for the purpose of worst-case estimation. Target diameters are set equal to the particular thickness.

In the MCNPX simulations, eight particle types are considered for the secondary radiation transport: neutrons (n), photons (p), protons (h), electrons (e), deuterons (d), tritons (t), He-3 ions (s), and alphas (a). Transport cut-off energies were set to their minimum values as described in the MCNPX manual [2]: 0 MeV (n), 1 keV (p), 1 MeV (h), e: 1 keV (e), 2 MeV (d), 3 MeV (t), 3 MeV (s), and 4 MeV (a). The following cross sections and tabulated models were used: ENDF60/Bertini INC model (n), MCPLIB02 (p), EL03 (e), Bertini INC model (h), and ISABEL model (d, t, s, a). A detailed description of the features of the FLUKA code and of the physics model embedded in can be found in [3]. In the FLUKA simulations the following secondary particles (down to the cut-off energy) were transported: n (10^{-14} GeV), p (1 keV), h (1 MeV), e (10 keV), muons (100 keV) and pions (100 keV).

The secondary particle fluence is recorded over a spherical surface “far” from the target surface at a distance of 5 m from the target centre. The angular scattering distribution relative to the direction of the proton beam incidence is divided into 10° intervals. The average particle fluence in each angular interval is multiplied by the square of the radius of the sphere to get the angular distributions of particle yields per steradian.

3 RESULTS AND DISCUSSION

3.1 Total Yields of Secondary Particles

The characterization of the secondary radiation for different targets is investigated by detecting the number, energy, and angular distribution of the emitted particle types. The total particle yields, i.e. the total number of particles leaving the target per incident proton, obtained by MCNPX and FLUKA are listed in Table II.

Table II. Total particle yields: comparison of MCNPX and FLUKA results for six investigated target materials

Target	n Yield		p Yield		h yield		e yield	
	MCNPX	FLUKA	MCNPX	FLUKA	MCNPX	FLUKA	MCNPX	FLUKA
Tiss.	0.21	0.20	0.26	0.24	0.0041	0.0035	0.0040	0.0052
Fe	0.81	0.73	0.82	0.79	0.0041	0.0030	0.0070	0.0116
Al	0.65	0.55	0.79	0.71	0.0035	0.0025	0.0079	0.0103
Cu	1.02	0.89	0.88	0.76	0.0036	0.0026	0.0065	0.0114
Steel	0.81	0.72	0.84	0.78	0.0043	0.0029	0.0075	0.0114
Conc.	0.40	0.35	0.40	0.33	0.0019	0.0016	0.0052	0.0066

For all targets the particle fluence is dominated by neutrons (n) and photons (p). Their contribution is up to one emitted particle per primary proton. MCNPX results seem to be generally higher (up to 20%) compared to FLUKA. The maximum neutron emission is found for the copper target being about a factor of five higher than for the soft tissue patient phantom. The absolute values of the reported target material yields should be handled with care because of their dependence on the chosen “thick” target dimensions and transport cut-off energies. For all investigated metal targets, the particle energy yields, i.e., the mean of the emitted particle energies per incident primary proton, are quite similar. For example, the MCNPX energy yields for irradiation of the iron target are 13.74 MeV (n), 1.20 MeV (p), 0.25 MeV (h), 0.01 MeV (e), 0.0003 MeV (d), 0.00004 MeV (a), 0.000005 (t), and 0.000005 MeV (s). In total, about 6% of the incoming proton energy of 250 MeV is leaving the iron target in form of secondary radiation. The total neutron yields were compared to the published results of Agosteo et al. [6] for the iron target (similar dimensions were chosen in the studies) and for 250 MeV proton beam energy. The differences to the literature values are +5% and -5%, for MCNPX and FLUKA respectively. In contrast to this good agreement, the results for the tissue target are deviating by more than a factor of two. No explanation for this disagreement has been found at this time.

3.2 Angular Distribution of Secondary Particles

The graphical representation of the angular distributions of the neutron and photon yields outside different targets as calculated by MCNPX can be seen in Fig. 1 and Fig. 2, respectively. The direction of incidence of the proton beam is indicated by an arrow pointing to the target which is located at the centre.

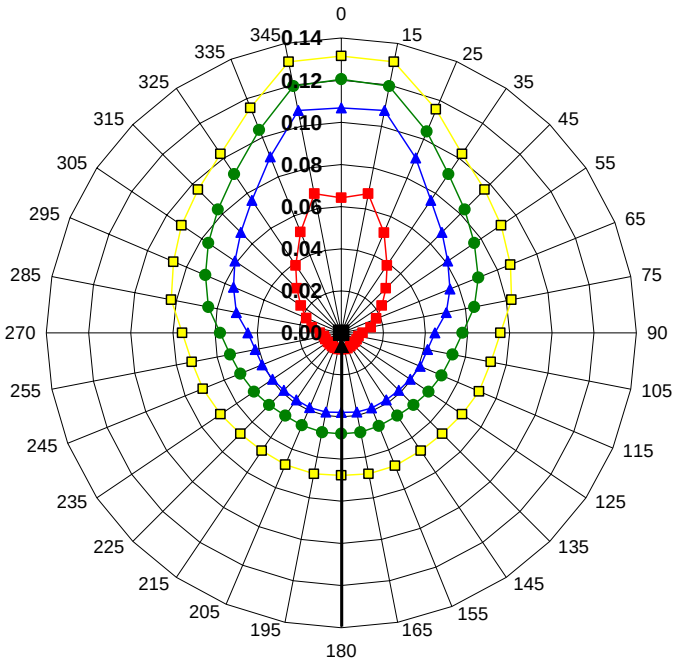

Figure 1. Angular distribution of the secondary neutron yield in units [1/sr/proton] for different targets: Tiss. (red ■), Fe (green ●), Al (blue▲), and Cu (yellow □)

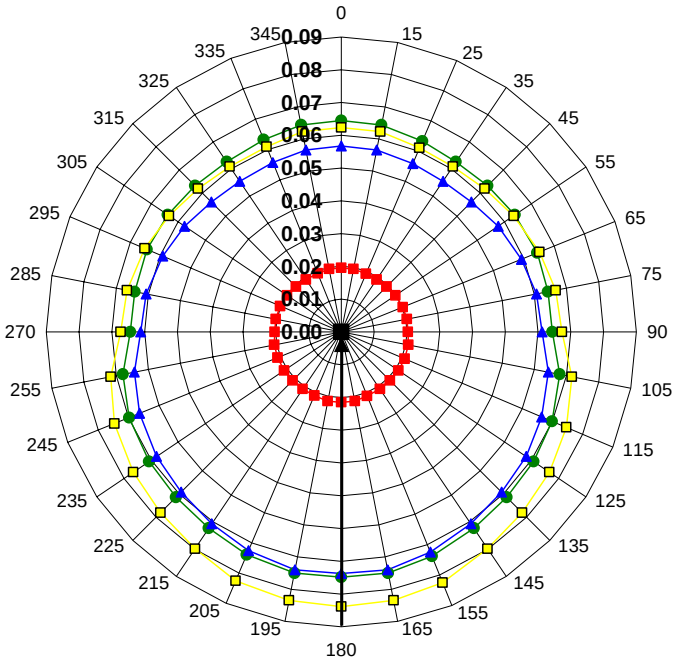

Figure 2. Angular distribution of the secondary photon yield in units [1/sr/proton] for different targets: Tiss. (red ■), Fe (green ●), Al (blue▲), and Cu (yellow □)

The values of the secondary neutron (n) and photon (p) emission results for the three main scattering angles are presented in Tables III and IV. The mean values of the FLUKA and the MCNPX results and the difference between the codes are listed for the six target materials. In the forward (0°-10°) direction, MCNPX neutron yields are generally lower, whereas in the lateral (80°-100°) and backward (170°-180°) directions, FLUKA provides the lower results. Differences between the two codes up to 40% are observed.

Table III. Angular neutron (upper) and photon (lower) yields in units [1/sr/proton]: for six target materials and for the three main scattering directions; mean value and difference between MCNPX and FLUKA

Target	n Yield (0°-10°)		n Yield (80°-100°)		n Yield (170°-180°)	
	mean	diff	mean	diff	mean	diff
Tiss.	8.16E-02	-35%	9.52E-03	14%	6.71E-03	40%
Fe	1.29E-01	-12%	5.44E-02	12%	4.61E-02	8%
Al	1.17E-01	-16%	4.03E-02	23%	3.45E-02	21%
Cu	1.38E-01	-9%	7.02E-02	17%	6.39E-02	12%
Steel	1.29E-01	-11%	5.39E-02	13%	4.60E-02	8%
Conc.	5.31E-02	-	2.60E-02	-	3.47E-02	-

Table IV. Angular photon yields in units [1/sr/proton]

Target	p Yield (0°-10°)		p Yield (80°-100°)		p Yield (170°-180°)	
	mean	diff	mean	diff	mean	diff
Tiss.	1.90E-02	6%	1.94E-02	10%	2.12E-02	3%
Fe	6.38E-02	2%	6.31E-02	4%	6.76E-02	24%
Al	5.66E-02	0%	5.61E-02	20%	6.43E-02	34%
Cu	6.13E-02	4%	6.02E-02	27%	7.08E-02	45%
Steel	6.35E-02	5%	6.21E-02	8%	6.69E-02	25%
Conc.	1.65E-02	-	2.84E-02	-	5.65E-02	-

3.3 Spectral Distribution of Secondary Particles

For calculating dose equivalent values in the environment of the target, it is necessary to measure the energy spectra of the secondary particle fields of the irradiated target. Neutrons are, in most cases, the dominant component of the secondary radiation as they carry the most (about 90% in forward direction) of the energy emitted by the target. For all investigated targets, Fig. 3 shows the forward (0°-10°) emitted spectral neutron yields calculated by MCNPX, i.e. the number of detected neutrons in the various energy intervals divided by the particular interval width and normalized to one steradian and one primary proton. It can be seen, that there are two kinds of secondary neutron spectra, i.e. the neutron spectra of the three metal targets clearly differ from the tissue and concrete spectra especially in the energy region below about 50 MeV.

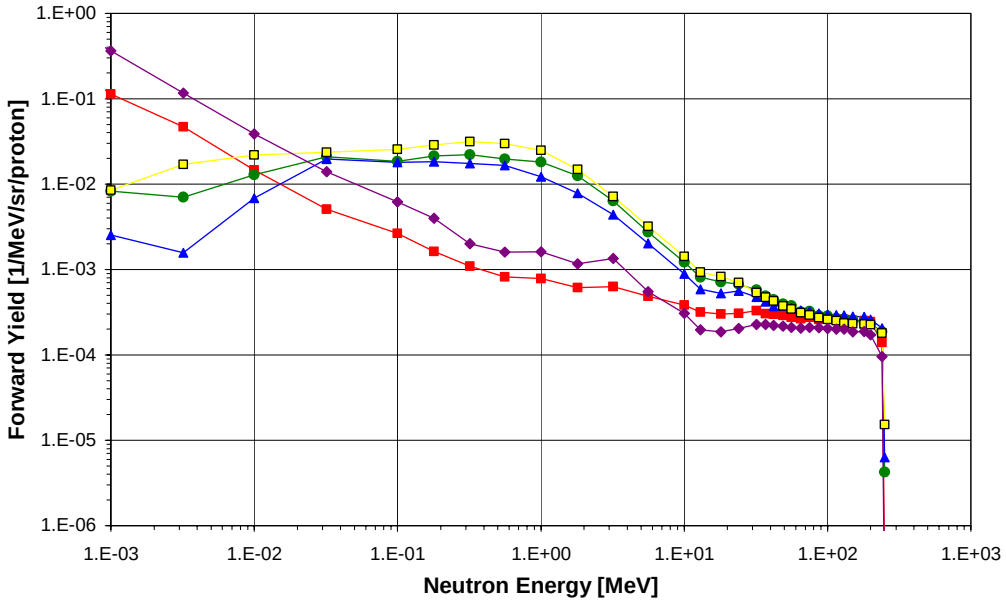

Figure 3. Spectral distribution of the secondary neutron yield in forward scattering direction for different targets: Tiss. (red ■), Fe (green ●), Al (blue▲), and Cu (yellow □), and Conc. (magenta ♦)

In Fig. 4 spectral neutron energy yields are presented for the iron target showing the change in the spectrum for different scattering angles. Neutrons with energies below about 10 MeV display a nearly isotropic angular distribution. Deep penetrating neutrons with energies up to 250 MeV are mainly scattered in forward direction causing the most important problems in shielding design.

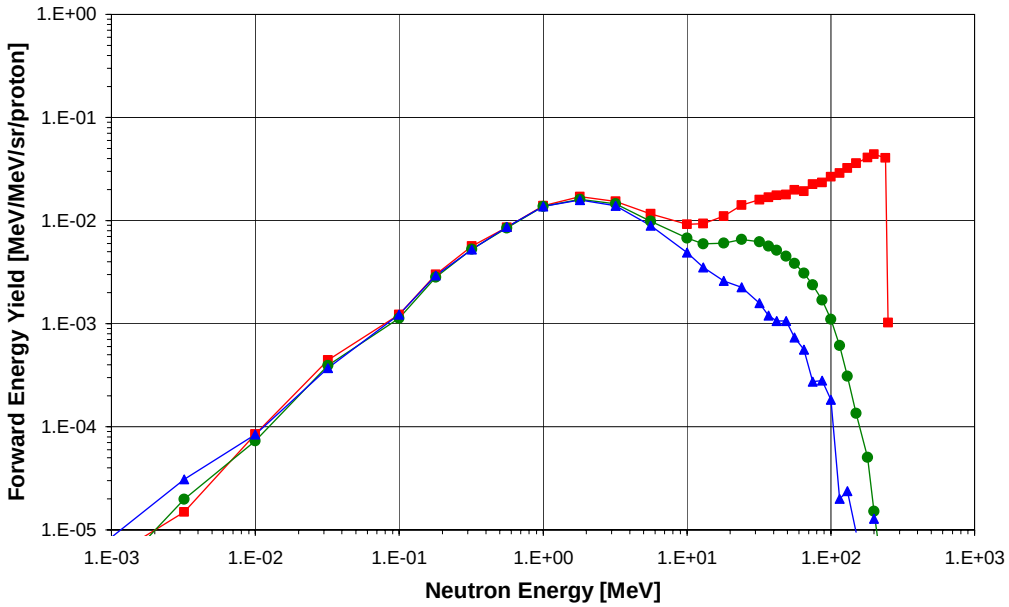

Figure 4. Spectral distribution of the secondary neutron energy yield for the iron target for the three main scattering directions: forward (red ■), lateral (green ●), and backward (blue▲)

3.4 Dose Distribution of Secondary Particles

The ambient dose equivalent values due to secondary particles are directly calculated in MCNPX from the angular fluence by applying fluence-to-dose conversion coefficients published by Ferrari and Pelliccioni [7]. Table V compares the H*(10) dose results for the three main scattering directions and for the six investigated thick targets. Therefore, the dose contribution of the three main particle types (n, p, and h) is summed up. The ambient dose equivalent per primary proton can be calculated by dividing the values of column one by the square of the actual distance. In column two, this is demonstrated for a target-detector-distance of 5 m. For the presented dose values of column three, a continuous proton beam current of 10^{10} protons/s (about 1.6 nA) is assumed. The minimum and maximum detected dose rates are 0.3 mSv/h and 6.9 mSv/h for the tissue target in backward scattering direction and for the copper target in forward scattering direction, respectively. The maximum dose rate in forward direction is predominantly due to secondary neutrons (97%) and to a lesser extent due to protons (2%) and photons (1%). The contributions of protons and photons to the minimum dose rate in backward direction are significantly higher, 9% and 6% respectively.

Listed dose values in column one of Table V are so-called source terms and can be used for analytical shielding calculations. A comparison of iron and copper target source terms for primary proton energies ranging from 100 MeV to 400 MeV to literature data can be found in [6]. Differences up to a factor of two may be explained by the use of different fluence-to-H*(10) conversion coefficients and different Monte Carlo codes, i.e. MCNPX and FLUKA in this work and the publication by Agosteo et al. Higher deviations especially for doses in lateral and backward directions require further investigations.

Table V. H*(10) ambient dose equivalent results: for six different target materials and for the three main scattering directions

Target	Angle	H*(10) r^2 [pSv cm^2/proton]	H*(10) 5 m [pSv/proton]	H*(10) 5 m & 1.6nA [mSv/h]
Tiss.	forward (0°-10°)	21.69	8.68E-05	3.1
	lateral (80°-100°)	4.22	1.69E-05	0.6
	back (170°-180°)	2.36	9.44E-06	0.3
Fe	forward (0°-10°)	43.69	1.75E-04	6.3
	lateral (80°-100°)	23.85	9.54E-05	3.4
	back (170°-180°)	19.93	7.97E-05	2.9
Al	forward (0°-10°)	37.68	1.51E-04	5.4
	lateral (80°-100°)	18.04	7.22E-05	2.6
	back (170°-180°)	15.04	6.02E-05	2.2
Cu	forward (0°-10°)	48.05	1.92E-04	6.9
	lateral (80°-100°)	30.29	1.21E-04	4.4
	back (170°-180°)	26.77	1.07E-04	3.9
Steel	forward (0°-10°)	44.25	1.77E-04	6.4
	lateral (80°-100°)	23.83	9.53E-05	3.4
	back (170°-180°)	19.86	7.95E-05	2.9
Conc.	forward (0°-10°)	16.52	6.61E-05	2.4
	lateral (80°-100°)	7.98	3.19E-05	1.1
	back (170°-180°)	10.21	4.08E-05	1.5

3.5 Target Thickness and Diameter Variations

The influence of the geometrical target specifications on the secondary radiation emission is briefly investigated for cylindrical copper targets. The simulation of the 250 MeV proton beam irradiation is carried out for four different values for the target thickness (0.3 cm, 3 cm, 7.5 cm, 30 cm) and two different target diameters (7.5 cm, 37.5 cm). The main focus is concentrated on the neutron fluence results in forward scattering direction. For a target diameter of 7.5 cm, reducing the target thickness to 3 cm and 0.3 cm reduces the neutron fluence by a factor of 1.4 and 13, respectively. Is the target diameter chosen to be 37.5 cm instead, then these neutron fluence reductions increase to a factor of 2.0 and 21, respectively.

For the 30 cm thick target the forward emitted fluence is approximately reduced by one order of magnitude. However, the maximum emission showed to be off-axis, e.g. about 60° for the neutron fluence exiting the 7.5 cm diameter target because of the small diameter compared to the target thickness. The resulting angular neutron and photon fluence distributions are presented in Fig. 5.

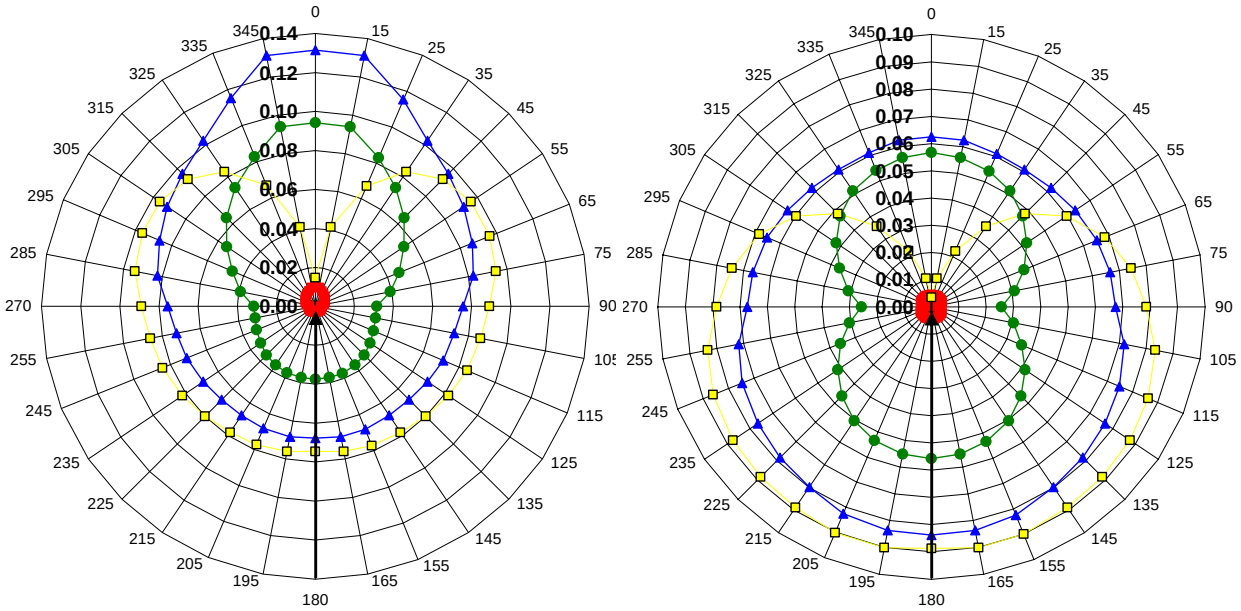

Figure 5. Angular distribution of the secondary neutron (left) and photon (right) yields in units [1/sr/proton] for Cu targets of 7.5 cm diameter and different thicknesses: 0.3 cm (red ■), 3 cm (green ●), 7.5 cm (blue▲), and 30 cm (yellow □)

Investigation of the photon fluence for these four different values for the target thickness gives comparable results. The maximum forward fluence is observed for a target thickness of 7.5 cm. For example, for the 37.5 cm diameter Cu target, reducing the thickness to 3.0 and 0.3 cm results in a lower forward scattered photon yield by factors of 1.5 and 23, respectively. Proton yields in the forward direction in these cases, however, increase by more than four orders of magnitude when the target thickness is changed from 7.5 cm to 3.0 or 0.3 cm. These are mainly due to unscattered protons from the original proton beam in the forward direction when the target thickness is well below the material's stopping range.

4 CONCLUSIONS

The secondary particle emission and resulting dose values in the unshielded environment of proton beam irradiated targets depend on a number of beam and target parameters. Only the highest available beam energies have to be considered in a worst case study. For radiation protection purposes two target material types can be distinguished, i.e. metal and tissue-

equivalent targets. Following the worst case approach, target dimensions comparable to the proton stopping range have to be chosen.

Comparing the total yield of different particle types, neutrons and photons have the highest yield up to one emitted particle per incident source proton. Weighting with the particular particle energies, the total energy yield originates mainly from neutrons whereas the forward scattering contributions are lower for photons, protons, and electrons by one, two, and three orders of magnitude, respectively.

In the present study, the differences between the two Monte Carlo codes, MCNPX and FLUKA, are up to 20% in the total yields and up to 40% in the angular yields. In contrast, statistical uncertainties of the simulation results can be neglected. The reported differences seem to be quite high but may be acceptable as compared to measurement uncertainties. The differences can be used as estimates of a combined Monte Carlo simulation uncertainty including mainly uncertainties due to interaction cross-sections and physics models. The results of this work point out the importance of quality assurance arrangements for computer simulations in radiation dosimetry, e.g. using a second Monte Carlo code, additional analytical calculation methods, verification measurements, and comparisons to literature results.

5 REFERENCES

1. T. Auberger, E. Griesmayer, *The MedAustron design study*, (in German), Fotec Forschungs- und Technologietransfer, ISBN 3-200-00141-0, Wiener Neustadt, Austria (2004).
2. L. S. Waters, “MCNPX 2.4.0 Monte Carlo N-particle transport code system for multiparticle and high energy applications”, *LA-CP-02-408 MCNPX user’s manual version 2.4.0*, Los Alamos National Laboratory, Los Alamos, New Mexico, USA (2002).
3. A. Fasso, A. Ferrari, J. Ranft, P. R. Sala, “FLUKA: Status and perspective for hadronic applications”, *Proceedings of the Monte Carlo 2000 Conference*, Lisbon, October 2000, Springer-Verlag Berlin, pp.955-960 (2001).
4. A. Brandl, C. Hranitzky, S. Rollet, “Shielding Variation Effects for 250 MeV Protons on Tissue Targets”, *ISRS-10 / RPS-2004 - 10th International Conference on Radiation Shielding and Radiation Protection*, Madeira, Portugal, 9-14 May 2004, to be published in Radiat. Prot. Dosim. (2005).
5. International Commission on Radiation Units and Measurements, “Stopping power ranges for protons and alpha particles”, *ICRU Report 49*, ICRU Publications, Bethesda, Maryland, USA (1993).
6. S. Agosteo, A. Fasso, A. Ferrari, P.R. Sala, M. Silari, “Double differential distributions and attenuation in concrete for neutrons produced by 100-400 MeV protons on iron and tissue targets”, Nucl. Instr. And Meth. In Phys. Res. **B 114**, pp.70-80 (1996).
7. A. Ferrari, M. Pelliccioni, “Fluence to dose equivalent conversion data and effective quality factors for high energy neutrons”, *Rad. Prot. Dosim.* **76(4)**, pp.215-224 (1998).